Figure 1. Effects of Hsp70 /Hsc70 on the levels of hERG-FLAG and its ubiquitination in HEK293 cells. Cells were transiently transfected with hERG-FLAG, pEGFP, and either Hsp70 **(A)** or Hsc70 **(C)**. HEK293 cells transfected with hERG-FLAG constructs were treated with either a scramble siRNA (mock) or siRNA against Hsp70 **(B)** or Hsc70 **(D)** (n=5 to 9). The amounts of plasmids (μg) are indicated in each **panel**. Shown are representative blots. Cell extracts were subjected to IB with indicated antibodies (n=4 to 11) **(left)** or anti-FLAG immunoprecipitates (IP) were subjected to IB with anti-ubiquitin or FLAG antibody (n=5 to 7) **(right)**.

Both Hsp70 and Hsc70 Associate With hERG-FLAG

To explore a biochemical basis for the opposite effects of Hsp70 and Hsc70, we examined their association with hERG by immunoprecipitation. The anti-FLAG immunoprecipitates (IPs) from hERG-expressing HEK293 cells contained endogenous Hsp70 and Hsc70 (Figure 5A). Both anti-Hsp70 and anti-Hsc70 IPs contained the 135-kDa immature form of hERG, but not the 155-kDa mature form, suggesting selective association of these chaperones with the immature form (Figure 5B). The specificity of Hsp70 and Hsc70 antibodies was confirmed by Western blotting using Hsp70 or Hsc70 recombinant proteins (Online Figure III, A).
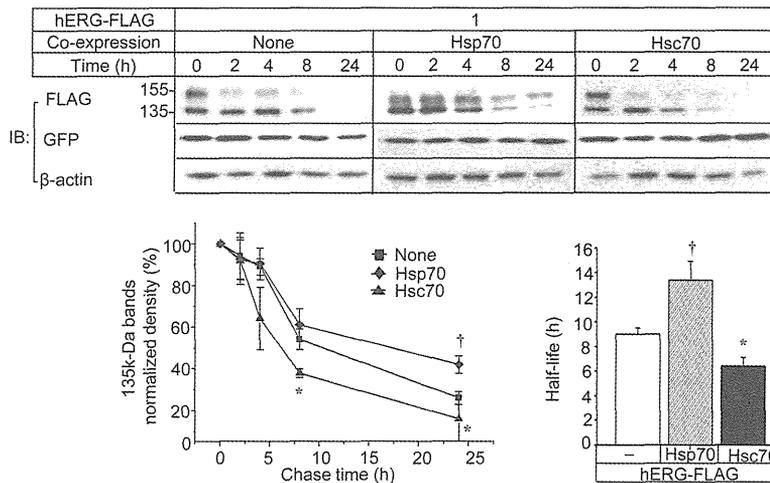
Figure 2. Degradation of hERG-FLAG proteins. HEK293 cells transiently expressing hERG-FLAG together with Hsp70 or Hsc70 were chased for the indicated time after addition of cycloheximide. Shown are the representative blot and time-dependent changes in the density of hERG-FLAG. The density of 135-kDa hERG-FLAG was normalized to the density at time 0 and β-actin. **Bar graph** shows half-life of hERG proteins. *$P<0.05$, †$P<0.01$ vs hERG-FLAG only (none) (n=6 to 7).

Coexpression of Hsp70 increased the levels of hERG-FLAG recovered by anti-FLAG. Cotransfection of Hsc70 with Hsp70 diminished the increases of hERG-FLAG in a dose-dependent manner (Figure 5C). Accordingly, the level of Hsp70 in anti-FLAG IPs was reduced by Hsc70, and this reduction was accompanied by an increase in the level of Hsc70 in the IPs (Figure 5D). These data suggested that Hsp70 and Hsc70 compete with each other in an interaction with hERG.

Regulation of Endogenous Mouse ERG and Cardiac Action Potential Duration by Hsp70 and Hsc70

To evaluate the physiological roles of Hsp70 and Hsc70 in the stability control of endogenous mouse (m)ERG, we used HL-1 mouse cardiomyocytes. In these cells, the anti-mERG antibody recognized an intense band at 155-kDa and a faint band at 135-kDa (Figure 6A). Immunoprecipitation with the anti-mERG antibody revealed an association of this protein with both Hsp70 and Hsc70 (Online Figure III, B). Hsp70 but neither Hsp90 nor Hsc70 was induced by a heat shock (HS) treatment at 42°C for 1 hour (Figure 6A), indicating selective induction of Hsp70 by HS. This increase in Hsp70 was accompanied by an apparent increase in the levels of both 135-kDa immature and 155-kDa mature forms of mERG. Under control conditions, anti-mERG IPs contained only Hsc70. After the HS, the same IPs contained Hsp70. Thus, HS-induced increase in Hsp70 switched the chaperone associated with mERG from Hsc70 to Hsp70 (Figure 6B).

siRNAs against Hsp70 were introduced into cells treated with the HS, because of the low level of Hsp70 in HL-1 cells. The siRNAs obviously decreased the level of Hsp70. The levels of both forms of mERG were also decreased compared with the levels in cells given a scrambled siRNA (Figure 6C, left). In contrast, siRNAs against Hsc70 increased the level of the Hsp70-mERG complex (Figure 6C, right). Hsp70 or Hsc70 was expressed in HL-1 cells using nucleofactor with transfection efficiency up to 90%. Hsp70 increased both forms of mERG, whereas Hsc70 diminished them (Figure 6D).

We next recorded I_{Kr} as the E4031-sensitive current in control and HS- treated HL-1 cells. The possible contamina-

tion of other voltage-dependent currents was minimized by adding 0.4μmol/L nisoldipine to bath solution to block $I_{Ca,L}$[20] and by setting a holding potential at -50mV to inactivate $I_{Ca,T}$ and to prevent activation of I_f.[20,21] Figure 7A shows whole-cell membrane currents recorded in HL-1. Depolarizing pulses activated time-dependent outward currents which increased with depolarization up to 0 mV (Control, None). The application of E4031 (10μmol/L) almost completely abolished the time-dependent outward current and the tail current (Control, E4031). E4031-sensitive current traces were obtained by digitally subtracting the current traces in the presence of E4031 from the traces in the absence ofE4031. The E4031-sensitive and -free currents have similar characteristics and current-voltage relationship, reflecting that I_{Kr} is the most prominent outward current in HL-1 cells. HS caused significant increases in both I_{Kr} peak and tail currents (Figure 7A and 7B).

Because the mERG current is responsible for repolarization of the cardiac action potential and I_{Kr} is the dominant outward current in HL-1cells,[18,22] we examined whether HS altered action potential duration (APD) in HL-1 cells. As shown in Figure 7C (a), the HS shortened APD at 90% repolarization (APD$_{90}$) without affecting resting membrane potentials. The APD$_{90}$ values in control and under HS treatment were 147.6±5.6 and 63.0±5.1 ms, respectively (Figure 7C, e). In accordance with these results, Hsp70 siRNA prolonged APD$_{90}$ as E4031 treatment, whereas Hsc70 siRNA shortened APD$_{90}$, regardless of the HS treatment (Figure 7C, b through d). Figure 7C (e) summarizes APD$_{90}$ values.

Because E4031 is a specific blocker of I_{Kr}, comparing the APD$_{90}$ to that with and without E4031 treatment (the ratio of APD$_{90}$ E4031/APD$_{90}$ control) clarifies the contribution of I_{Kr} to APD$_{90}$. As shown in Online Figure IV, HS treatment significantly increased the ratio of APD$_{90}$ E4031/APD$_{90}$ compared to that of control, whereas its effect was abolished by siRNA Hsp70. This indicated that HS-induced shortening of APD$_{90}$ was attributable to an increase of I_{Kr} via activation of Hsp70. Interestingly, siRNA against Hsc70 also significantly increased the ratio of APD$_{90}$ E4031/APD$_{90}$ control, suggesting that APD$_{90}$ may normally be under Hsc70 control.
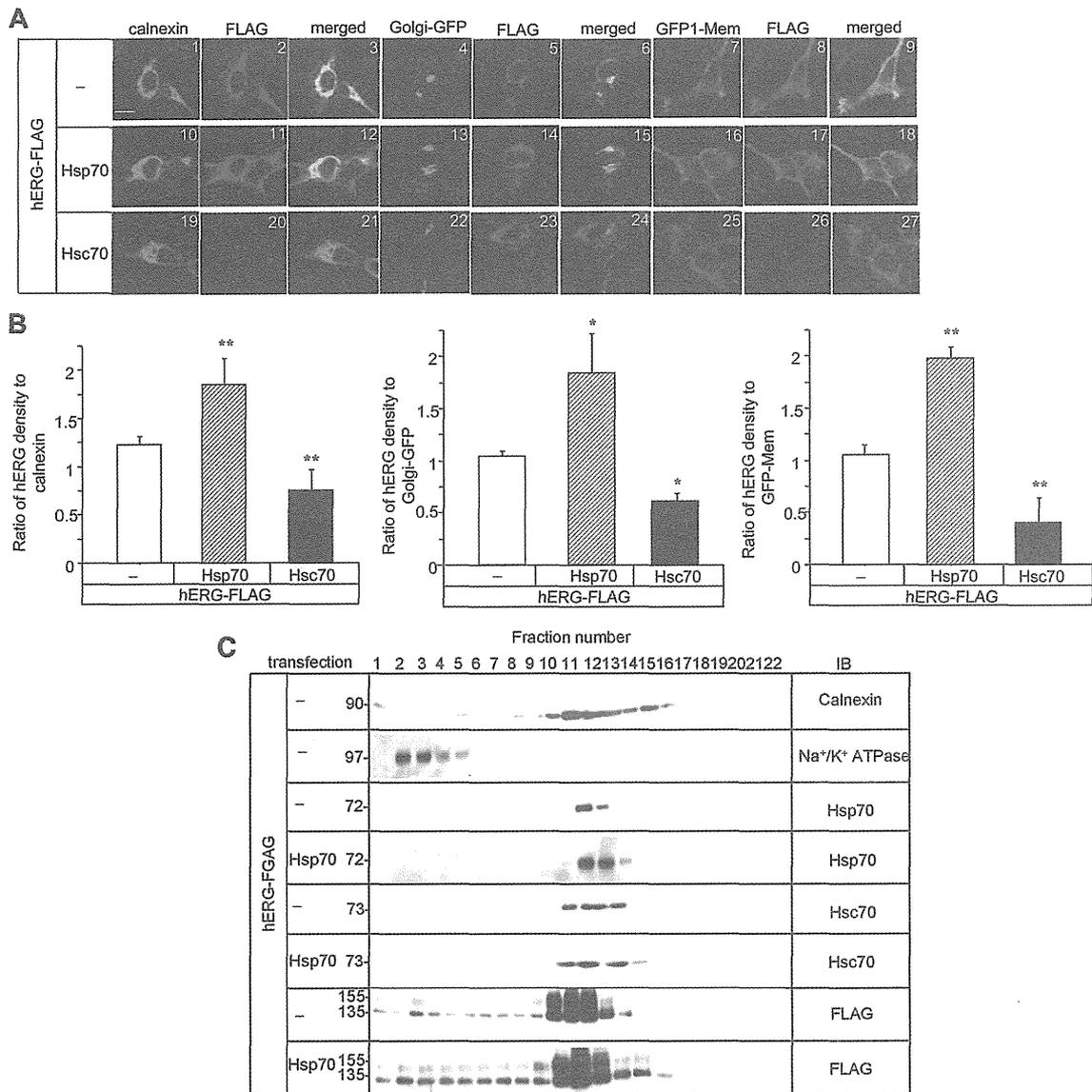
A

B

C

Figure 3. Intracellular localization of hERG-FLAG. A, Immunofluorescence of hERG-FLAG in HEK293 cells. Cells were transfected with hERG-FLAG together with pcDNA3 or Hsp70 or Hsc70 expression constructs. Parts of the cells were cotransfected with pAcGFP-Mem or Golgi-GFP. One set of cells was immunostained by calnexin **(green)**. All the cells were stained with anti-FLAG and Alexa Fluor 546–conjugated secondary antibody **(red)**. Shown are representative images obtained by a confocal microscope. Bar, 20 μm. **B,** Quantification of anti-FLAG immunoreactivity. Shown is the ratio of intensity for Alexa 546/calnexin, Golgi-GFP, or pAcGFP-Mem fluorescence. Each **column** represents the mean±SEM of 12 to 15 determinations. ******$P<0.01$, *****$P<0.05$ vs mock (none) (n=12 to 15). **C,** Cell fractionation. Whole-cell homogenates were prepared from HEK293 cells transiently expressing hERG-FLAG or with Hsp70 after 48 hours of transfection. The postnuclear supernatants were fractionated by a liner gradient of iodixanol. hERG-FLAG protein and various organelle markers were detected by IB analyses.

Stability Control of hERG Mutant Proteins by Hsp70 and Hsc70

Because mutations of hERG impair their stability, we examined binding activities of mutant hERG to Hsp70 and Hsc70. For this purpose, we engineered 10 kinds of mutant hERG proteins. The location of each missense mutation is depicted in Figure 8A (top). Figure 8A (bottom) shows representative IBs of cell lysates from HEK293 cells expressing either wild-type (WT) or various mutant hERG-FLAG. All of the mutant hERG gave only

the 135-kDa band. IP experiments showed that the mutants with mutations in intracellular domains preferentially associated with Hsc70; whereas those with mutations in the pore-region preferentially associated with Hsp70.

We then examined degradation of 2 kinds of mutant proteins, P596R, a mutation located in the pore-region, and F805C, an intracellular domain mutation. Chase experiments showed that F805C and P596R had half-life of 4.3 ± 1.5 hours and 7.4 ± 3.7 hours (n=5 to 7, $P<0.05$), respectively. Hsc70
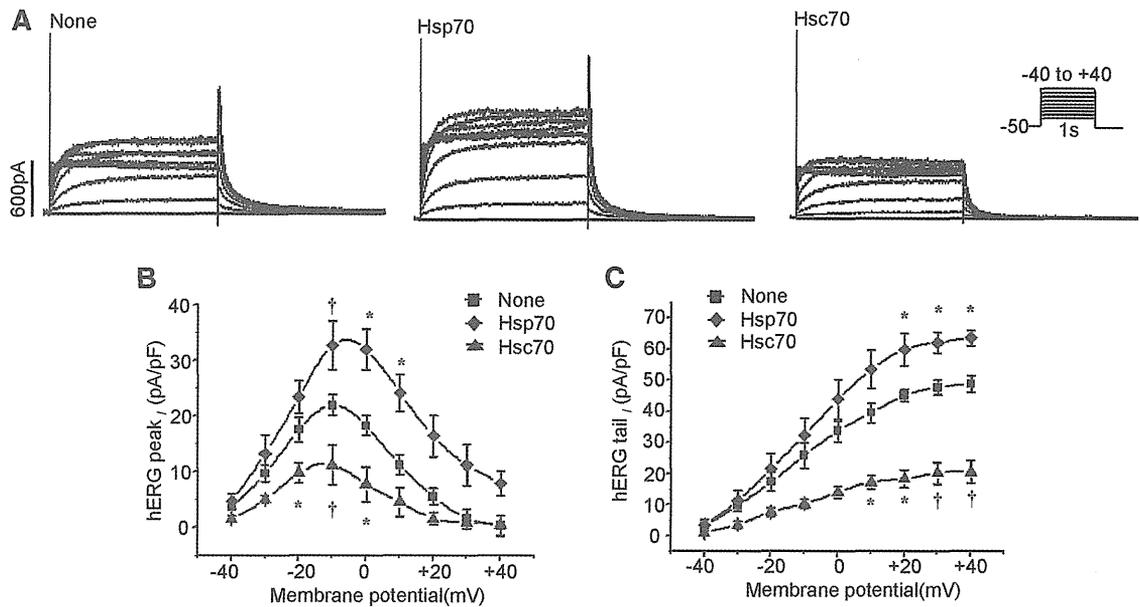
Figure 4. Effects of Hsp70/Hsc70 on hERG currents in HEK293 cells stably expressing hERG-FLAG. Representative current traces recorded from cells transfected with Hsp70 or Hsc70 or mock plasmid (none) **(A)**. The membrane potential was held at −50 mV, depolarized by 1-sec test pulses ranging from −40 to +40mV and then repolarized back to the holding potential for tail current measurement. Average current–voltage relationships of peak and tail currents are shown in **B** and **C**. Values represent means±SEM. Differences between the control and the group with Hsp70 or Hsc70 were tested statistically. *$P<0.05$, †$P<0.01$ vs none (n=17 to 19).

siRNA prolonged half-life of both mutants. However, the effects were more prominent in F805C mutant (76% increase) than in P596R (29% increase) (Figure 8B).

Because HS could decrease the association of Hsc70 with hERG, we examined effects of HS on the stability of WT and 10 kinds of mutant hERG in transfected HL-1 cells. On IBs, WThERG-FLAG gave 2 intense bands, whereas the mutant proteins gave only a faint 135-kDa band (Figure 8C). HS dramatically increased not only the levels of the mature form of WT but also those of mutant hERG, and again this effect of HS was more prominent in those mutant proteins with intracellular domain mutations than those mutant located in the pore-region.

Previous studies have shown that specific hERG mutants can be stabilized by incubating the cells at low temperature.[4] We examined whether expression of hERG and its association with Hsp70 and Hsc70 were affected by hypothermia. WThERG-FLAG, P596R-FLAG, F805C-FLAG, R752W-FLAG and G601S-FLAG were transfected into HEK293 cells, then the cells were cultured at 37°C for 24 hours then at 27°C for 24 hours. The hypothermia increased not only the levels of WT mature and immature forms but also the levels of 2 forms of mutants (Figure 8D). IP experiment showed that the hypothermia decreased the association of mutant hERG with Hsc70 but not with Hsp70, suggesting that both WT and
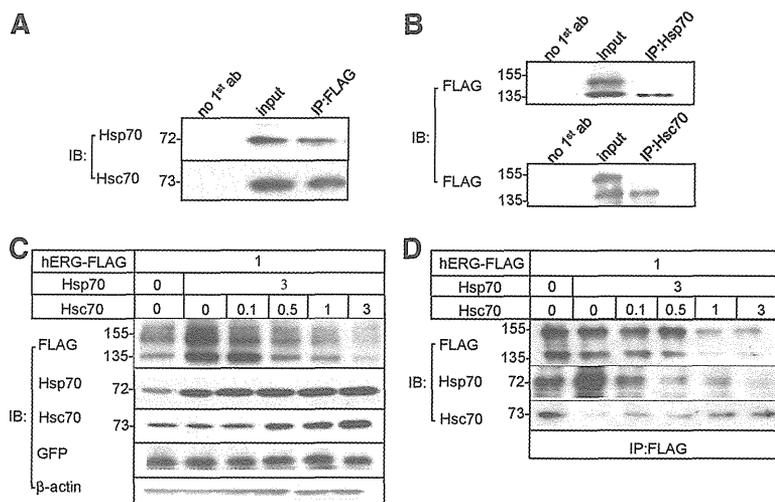

Figure 5. Effects of Hsc70 on Hsp70-induced increase of hERG-FLAG. A, Association of hERG-FLAG with Hsp70 or Hsc70. Anti-FLAG IPs from HEK293 cells transiently expressing hERG-FLAG were subjected to IB with anti-Hsp70 or Hsc70 antibody. No 1st ab represents a negative control with no primary antibody added and input is positive control. **B,** Anti-Hsp70 or Hsc70 IPs from HEK293 cells transiently expressing hERTG-FLAG were subjected to IB with anti-FLAG. **C,** HEK293 cells were transfected with indicated plasmids (μg). Whole-cell lysates were subjected to IB with indicated antibodies (n=4 to 6). **D,** Anti-FLAG IPs were subjected to IB with either anti-FLAG, Hsp70, or Hsc70 (n=6 to 7).
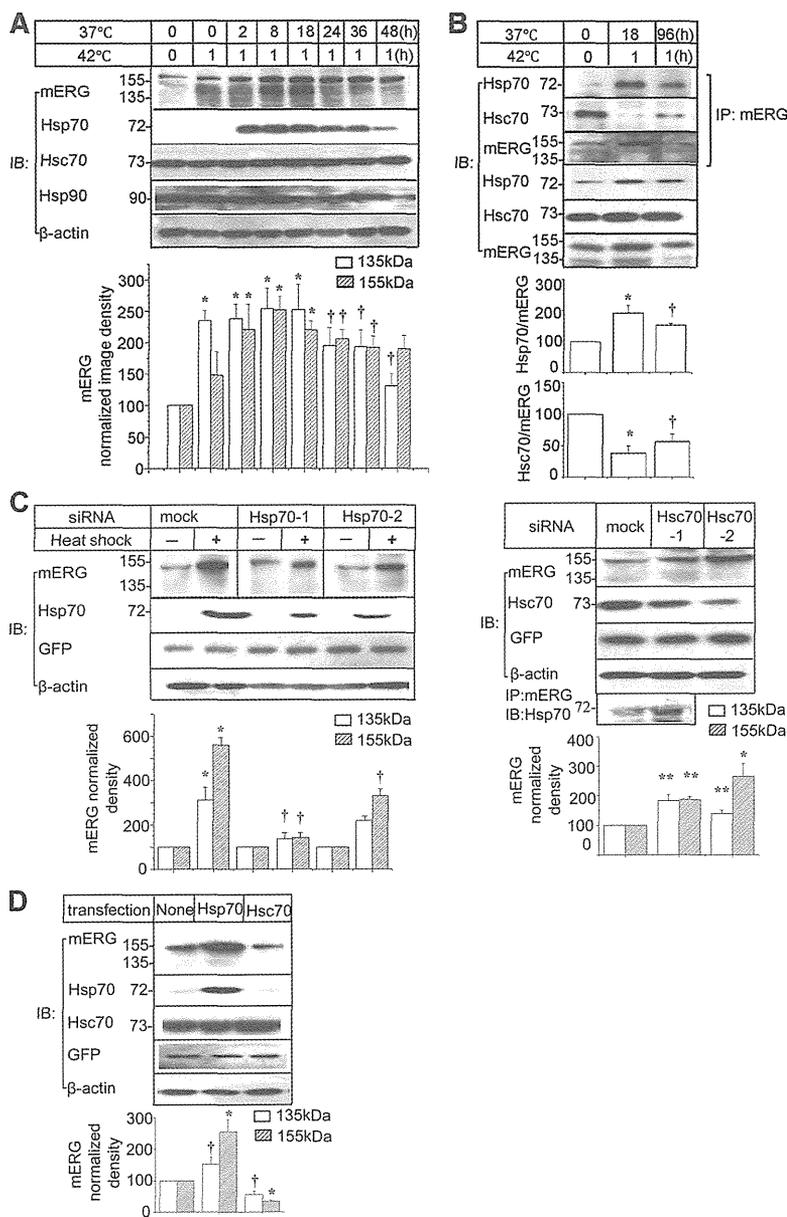
Figure 6. Effects of HS on the level of endogenous mouse ERG (mERG) in HL-1 cells. **A,** Cells were given a heat shocked at 42°C for 1 hour. The cells were recovered at the indicated times and analyzed by IB with indicated antibodies. Image densities of the immature and mature forms of mERG bands normalized to mERG expression levels in non-HS control cells ($n=6$ to 7, *$P<0.01$, †$P<0.05$ vs non-HS). **B,** Association of mERG with Hsp70 or Hsc70 was detected by IB. Anti-mERG IPs was subjected to IB. **Bar graphs** show the levels of Hsp70 or Hsc70 associated with mERG ($n=4$ to 5, *$P<0.01$, †$P<0.05$ vs non-HS group). **C,** HL-1 cells were transfected with a scramble siRNA (mock) or siRNAs against mouse Hsp70 **(left)** or Hsc70 **(right).** The levels of mERG, Hsp70, and Hsc70 were analyzed by IB. Image density of mERG were quantified and normalized to mERG levels in the cells with a scramble siRNA ($n=5$ to 6, *$P>0.01$, **$P>0.05$ vs non-HS; †$P>0.05$ vs with a scramble siRNA with HS). **D,** Effects of Hsp70 or Hsc70 on endogenous mERG. HL-1 cells were transfected either with pcDNA3, Hsp70, or Hsc70 plasmid. Cell lysate was subjected to IB with the indicated antibodies ($n=5$ to 7, *$P<0.01$; †$P<0.05$ vs none).

mutant hERG proteins were stabilized because of disassociation from Hsc70 at low temperature.

Discussion

In the present study, we found that Hsp70 and Hsc70 exert opposite effects on the stability of hERG, ie, Hsp70 stabilized hERG, whereas Hsc70 destabilized it. The main site of action of these chaperones appeared to be the ER. Both Hsp70 and Hsc70 could associate with hERG and the stability control appeared to be a direct consequence of their association. We have also shown that the levels of these chaperones influenced cardiac APD. Evidence was also presented that disease-causing missense mutations of hERG alter its association with these chaperones.

Hsp70 and Hsc70 Exert Opposite Effects on the Stability of hERG

Hsp70 could be induced by HS and cellular stress, whereas Hsc70 is constitutively expressed.[23] These 2 proteins have a high degree of sequence homology and have been believed to be functionally interchangeable.[24–26] This is the first report to demonstrate that Hsp70 and Hsc70 exert opposite effects on the stability of hERG protein through their association with the immature form. In general, Hsp70 acts on nascent and newly synthesized proteins to hold them in a state competent for proper folding.[11] In contrast, Hsc70 associates with newly synthesized proteins to promote their proteasomal degradation. This effect of Hsc70 has been demonstrated for
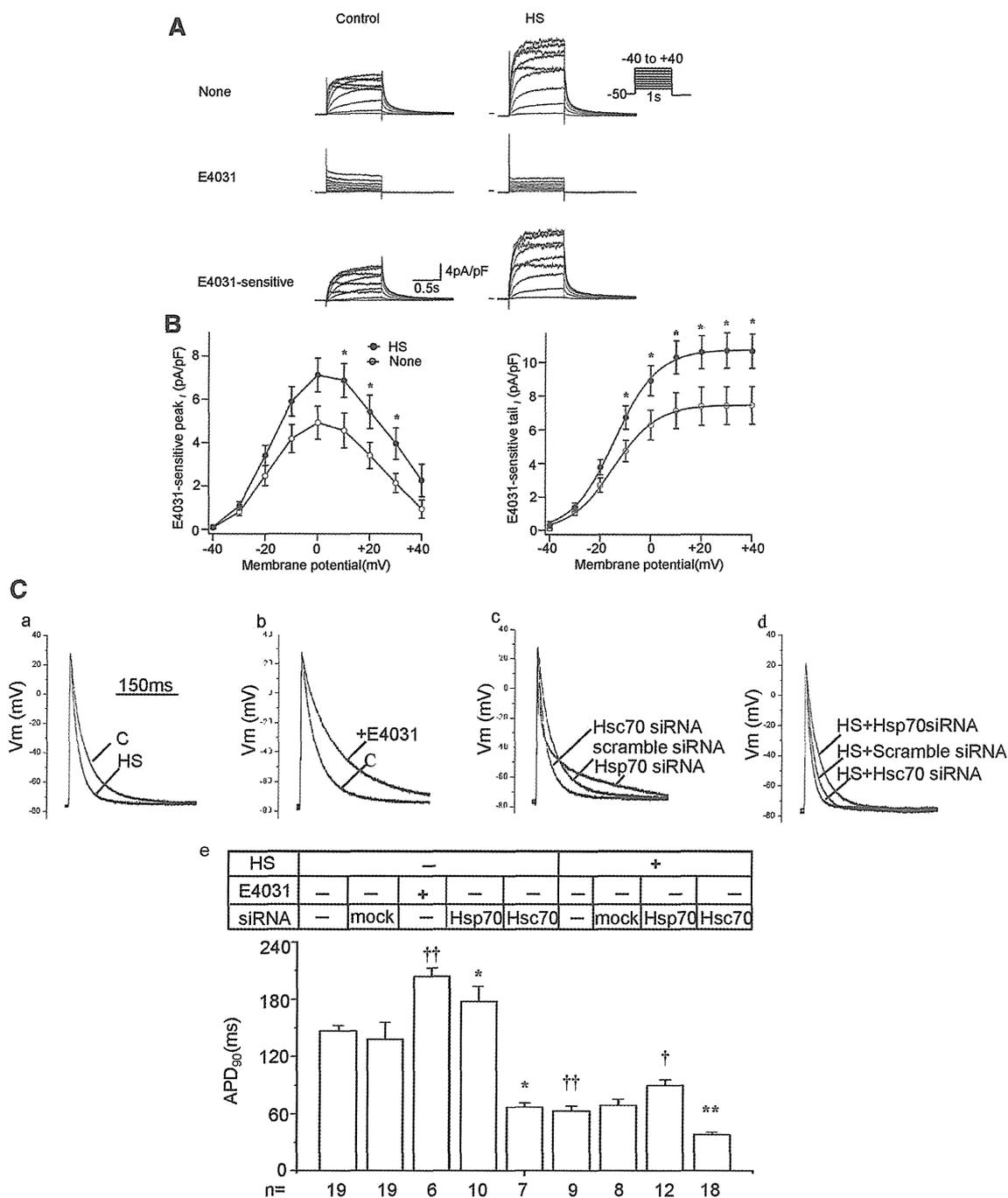
Figure 7. Effects of HS on E4031-sensitive currents and APD. A, Whole-cell membrane currents were recorded from a single HL-1 cell before (none) and after application of 10 μmol/L E4031. E4031-sensitive currents were obtained by digital subtraction. Current recordings were performed 24 hours after HS treatment at 42°C for 1 hour. B, Current–voltage relationships of the peak and tail of the E4031-sensitive currents (n=16, *P<0.05 vs none). C, Action potentials were recorded 24 hours after transfection of a scramble siRNA (mock) or a siRNA against Hsp70 or Hsc70 in the absence or presence of 10 μmol/L E4031. Representative action potentials are shown (a through d). APD$_{90}$ values are summarized as a bar graph (e), and statistically evaluated: ††P<0.01 vs non-HS; *P<0.01 vs a scramble siRNA control non-HS; †P<0.05, **P<0.01 vs a scramble siRNA with HS treatment.
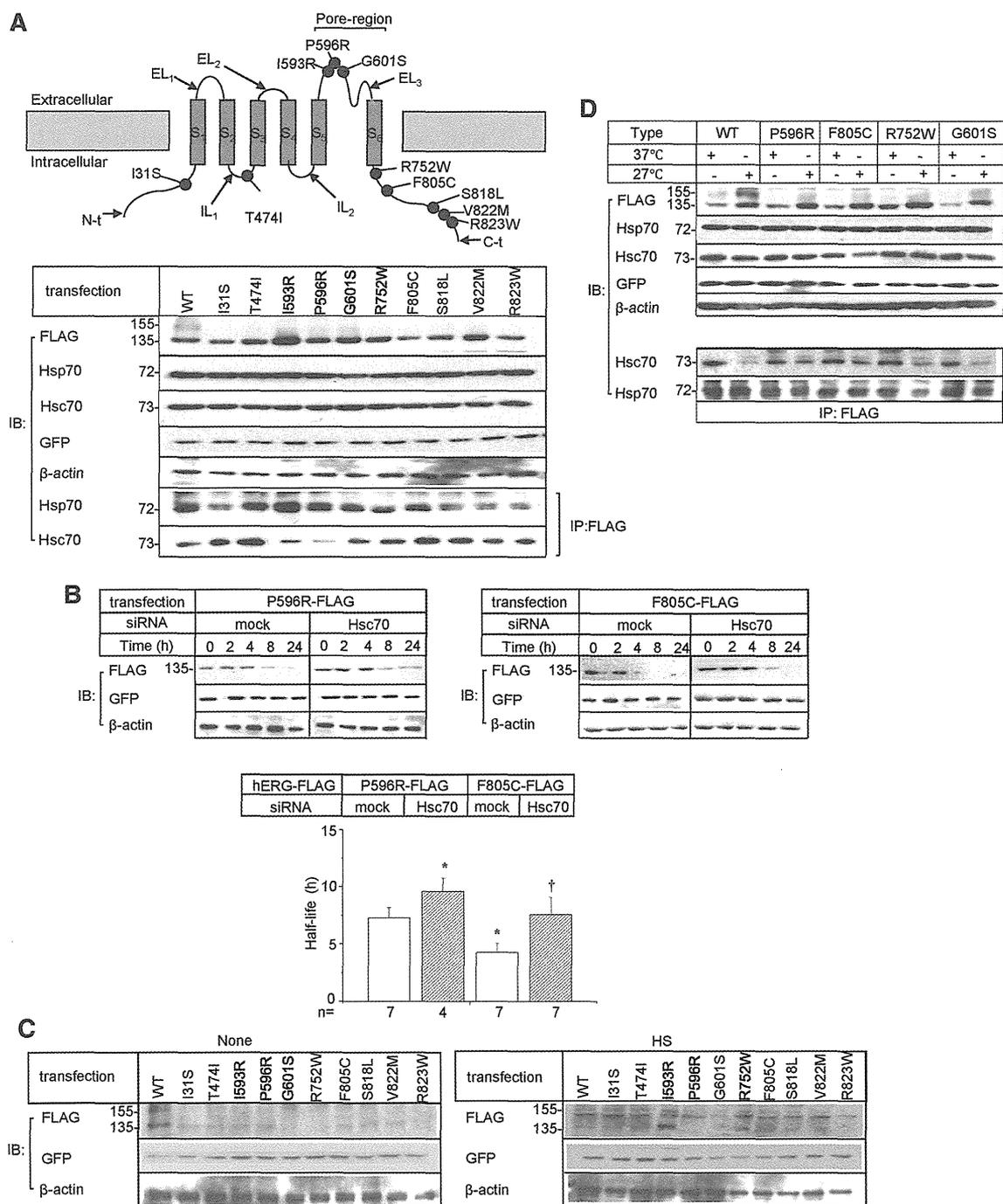
Figure 8. Effects of Hsp70 and Hsc70 on mutant hERG-FLAG. A, Top, Locations of LQT2-associated 10 mutations. **Black circles** indicate the locations of 10 missense mutations. The **arrows** point N terminus (N-t), intracellular loop (IL), extracellular loop (EL), and C terminus (C-t), respectively. WT hERG-FLAG and 10 kinds of mutant hERG-FLAG were transfected into HEK293 cells. Cell lysates or anti-FLAG IPs were subjected to IBs with indicated antibodies **(bottom). B,** Degradation of mutant hERG-FLAG. P596R-FLAG or F805C hERG-FLAG was transfected in HEK293 cells either with a scramble siRNA (mock) or an siRNA against Hsc70. Cells were chased for the indicated times after the addition of cycloheximide. Shown are representative Western blot with the indicated antibodies. Bar graphs summarize the half-life of 2 missense mutant hERG-FLAG. *$P<0.05$ vs P596R-FLAG with a scramble siRNA; †$P<0.05$ vs F805C-FLAG with a scramble siRNA. **C,** WT and mutant hERG-FLAG were transfected into HL-1 cell and the cells were given 1 hour of HS treatment at 42°C. Cell lysates were subjected to IB with indicated antibodies (n=4). **D,** Effects of hypothermia on WT and mutant hERG. Each construct was transfected into HEK293 cells. The cells were cultured at 37°C for 24 hours then at 27°C for 24 hours. The whole-cell lysates or anti-FLAG IPs were analyzed by IB with indicated antibodies (n=5 to 6).

CFTR,[27–29] murine epithelial sodium channel,[13] and ASIC$_2$ (acid-sensing ion channels).[30] Our findings are in agreement with those previous studies and presented evidence that Hsp/Hsc70 association with hERG is regulated by the cellular levels of these 2 chaperones (Figure 5C and 5D).

Hsp70/Hsc70 Controlled the Level of Endogenous mERG and the Cardiac APD

In this study, we identified that E4031-sensitive currents are the predominant component of the outward currents and show essentially the same characteristics as I_{Kr} in HL-1 murine cardiomyocytes. We demonstrated, for the first time, that HS was able to increase I_{Kr} and shorten cardiac APD. Under control conditions, Hsc70 associated with mERG to reduce the cellular level of mERG. HS- induced Hsp70 increases Hsp70-mERG complexes, causing an increase in the cellular level of mERG. The level of mERG is well known to regulate the activity of I_{Kr}[31] and I_{Kr} regulates cardiac APD, especially in mouse atrial myocytes,[19,32] which is one of the major factors to determine the QT interval.[22] E4031-induced prolongation of APD$_{90}$ was more remarkable in the cells treated with HS than in the control cells, indicating that the increased I_{Kr} contributes to acceleration of repolarization by HS through increases in Hsp70-mERG complex associated with decreases of Hsc70-mERG complex. These data strongly suggest that Hsp70/Hsc70 plays a pivotal role in controlling APD in cells treated with HS. Our findings might explain fever-induced shortening of the QT interval.[33,34] Interestingly, siRNA knockdown of Hsc70 shortened APD in HL-1 cells, indicating that Hsc70 is able to regulate APD under physiological conditions. These results are in accordance with antiarrhythmic effects of augmented expression of hERG that have been reported in rabbit ventricular primary culture and a transgenic mice model.[35,36] In both cases, hERG expression resulted in significant shortening of APD and decreased the incidence of early afterdepolarizations.

Stability Control of hERG Mutant Proteins by Hsp70 and Hsc70

Most of LQT2 missense mutations decrease the stability of hERG.[4] This instability has been associated with increased association with Hsp70/ Hsc70, which have been suggested to play similar function.[8] We found that the association of Hsp70 and Hsc70 with mutant channels depended on the nature of the mutation. The level of Hsc70-F805C hERG complexes was higher than that of Hsc70–P596R hERG complexes resulting in a shorter half- life of F805C hERG proteins. The F805C mutant yielded smaller hERG currents than the P596R mutant.[4] Silencing Hsc70 prolonged the half-life of both mutant proteins but more predominantly in F805C, suggesting that Hsc70 determines degradation of their immature forms, especially those with the intracellular mutations.

Accordingly, HS promoted the maturation of mutant hERGs with mutations in intracellular domains rather than those in pore-region. It is conceivable that the HS-induced Hsp70 causes a disassociation of Hsc70 from mutant hERGs and increases the level of Hsp70-hERG complexes. hERG proteins contain a PAS (Per, Arnt, and Sim) domain on their N terminus and a cNBD domain on their C terminus; both of them may be targeted by

cytosolic chaperones.[8] LQT2 mutations located in the N or C terminus might interfere the association of chaperones.[5] Ficker E et al reported decreased association of WT and mutant with Hsp70 /Hsc70 and increased hERG with reduced temperature.[8] We detected association of Hsp70 or Hsc70 with hERG separately and found that hypothermia decreased the level of Hsc70 associated with hERG, whereas it unaltered the level of Hsp70. Thus, the degradation of immature form of both WT and mutant hERG proteins was prevented by disassociation of Hsc70 under hypothermia. The biophysical characteristics of mutant hERG may be comparable with CFTRΔ508, a trafficking-deficient mutant. CFTRΔ508 can be rescued by Hsp70 and low-temperature culturing.[37,38] Both HS and low temperature result in disassociation of Hsc70 from mutant hERG proteins and stabilization of the immature form. Our data raise the possibility that Hsc70 and Hsp70 may be a target in the treatment of LQT2 which results from missense hERG mutations.

Disclosures

None.

References

1. Sanguinetti MC, Jiang C, Curran ME, Keating MT. A mechanistic link between an inherited and an acquired cardiac arrhythmia: HERG encodes the I_{Kr} potassium channel. *Cell.* 1995;81:299–307.
2. Sanguinetti MC, Tristani-Firouzi M. hERG potassium channels and cardiac arrhythmia. *Nature.* 2006;440:463–469.
3. Kiehn J, Lacerda AE, Wible B, Brown AM. Molecular physiology and pharmacology of HERG. Single-channel currents and block by dofetilide. *Circulation.* 1996;94:2572–2579.
4. Anderson CL, Delisle BP, Anson BD, Kilby JA, Will ML, Tester DJ, Gong Q, Zhou Z, Ackerman MJ, January CT. Most LQT2 mutations reduce Kv11.1 (hERG) current by a class 2 (trafficking-deficient) mechanisms. *Circulation.* 2006;113:365–373.
5. Thomas D, Kiehn J, Katus HA, Karle CA. Defective protein trafficking in hERG-associated hereditary long QT syndrome (LQT2): molecular mechanisms and restoration of intracellular protein processing. *Cardiovasc Res.* 2003;60:235–241.
6. Gong Q, Keeney DR, Molinari M, Zhou Z. Degradation of trafficking-defective long QT syndrome type II mutant channels by the ubiquitin-proteasome pathway. *J Biol Chem.* 2005;280:19419–19425.
7. Gong Q, Anderson CL, January CT, Zhou Z. Role of glycosylation in cell surface expression and stability of HERG potassium channels. *Am J Physiol Heart Circ Physiol.* 2002;283:H77–H84.
8. Ficker E, Dennis AT, Wang L, Brown AM. Role of the cytosolic chaperones Hsp70 and Hsp90 in maturation of the cardiac potassium channel HERG. *Circ Res.* 2003;92:87–100.
9. Petrecca K, Atanasiu R, Akhavan A, Shrier A. N-linked glycosylation sites determine HERG channel surface membrane expression. *J Physiol.* 1999;515:41–48.
10. Jakob U, Gaestel M, Engel K, Buchner J. Small heat shock proteins are molecular chaperones. *J Biol Chem.* 1993;268:1517–1520.
11. Hartl FU, Hayer-Hartl M. Molecular chaperones in the cytosol: from nascent chain to folded protein. *Science.* 2002;295:1852–1858.
12. Walker VE, Atanasiu R, Lam H, Shrier A. Co-chaperone FKBP38 promotes HERG trafficking. *J Biol Chem.* 2007;282:23509–23516.
13. Goldfarb SB, Kashlan OB, Watkins JN, Suaud L, Yan W, Kleyman TR, Rubenstein RC. Differential effects of Hsc70 and Hsp70 on the intracellular trafficking and functional expression of epithelial sodium channels. *Proc Natl Acad Sci U S A.* 2006;103:5817–5822.

14. Kato M, Ogura K, Miake J, Sasaki N, Taniguchi S, Igawa O, Yoshida A, Hoshikawa Y, Murata M, Nanba E, Kurata Y, Kawata Y, Ninomiya H, Morisaki T, Kitakaze M, Hisatome I. Evidence for proteasomal degradation of Kv1.5 channel protein. *Biochem Biophys Res Commun*. 2005;337: 343–348.

15. Tanaka H, Miake J, Notsu T, Sonyama K, Sasaki N, Iitsuka K, Kato M, Taniguchi S, Igawa O, Yoshida A, Shigemasa C, Hoshikawa Y, Kurata Y, Kuniyasu A, Nakayama H, Inagaki N, Nanba E, Shiota G, Morisaki T, Ninomiya H, Kitakaze M, Hisatome I. Proteasomal degradation of Kir6.2 channel protein and its inhibition by a Na+ channel blocker aprindine. *Biochem Biophys Res Commun*. 2005;331:1001–1006.

16. Hirota Y, Kurata Y, Kato M, Notsu T, Koshida S, Inoue T, Kawata Y, Miake J, Bahrudin U, Li P, Hoshikawa Y, Yamamoto Y, Igawa O, Shirayoshi Y, Nakai A, Ninomiya H, Higaki K, Hiraoka M, Hisatome I. Functional stabilization of Kv1.5 protein by Hsp70 in mammalian cell lines. *Biochem Biophys Res Commun*. 2008;372:469–474.

17. Koshida S, Kurata Y, Notsu T, Hirota Y, Kuang TY, Li P, Bahrudin U, Harada S, Miake J, Yamamoto Y, Hoshikawa Y, Igawa O, Higaki K, Soma M, Yoshida A, Ninomiya H, Shiota G, Shirayoshi Y, Hisatome I. Stabilizing effects of eicosapentaenoic acid on Kv1.5 channel protein expressed in mammalian cells. *Eur J Pharmacol*. 2009;604:93–102.

18. Claycomb WC, Lanson NA Jr, Stallworth BS, Egeland DB, Delcarpio JB, Bahinski A, Izzo NJ Jr. HL-1 cells: a cardiac muscle cell line that contracts and retains phenotypic characteristics of the adult cardiomyocyte. *Proc Natl Acad Sci U S A*. 1998;95:2979–2984.

19. Toyoda F, Ding WG, Zankov DP, Omatsu-Kanbe M, Isono T, Horie M, Matsuura H. Characterization of the rapidly activating delayed rectifier potassium current, I (Kr), in HL-1 mouse atrial myocytes. *J Membr Biol*. 2010;235:73–87.

20. Xia M, Salata JJ, Figueroa DJ, Lawlor AM, Liang HA, Liu Y, Connolly TM. Functional expression of L- and T-type Ca2+ channels in murine HL-1 cells. *J Mol Cell Cardiol*. 2004;36:111–119.

21. Sartiani L, Bochet P, Cerbai E, Mugelli A, Fischmeister R. Functional expression of the hyperpolarization-activated, non-selective cation current I(f) in immortalized HL-1 cardiomyocytes. *J Physiol*. 2002;545:81–92.

22. Tan HL, Hou CJ, Lauer MR, Sung RJ. Electrophysiologic mechanisms of the long QT interval syndromes and torsade de pointes. *Ann Intern Med*. 1995;122:701–714.

23. Cvoro A, Korac A, Matic G. Intracellular localization of constitutive and inducible heat shock protein 70 in rat liver after in vivo heat stress. *Mol Cell Biochem*. 2004;265:27–35.

24. Takayama S, Xie Z, Reed JC. An evolutionarily conserved family of Hsp70/Hsc70 molecular chaperone regulators. *J Biol Chem*. 1999;274: 781–786.

25. Brown CR, Martin RL, Hansen WJ, Beckmann RP, Welch WJ. The constitutive and stress inducible forms of hsp 70 exhibit functional sim-

26. Freeman BC, Morimoto RI. The human cytosolic molecular chaperones hsp90, hsp70 (hsc70) and hdj-1 have distinct roles in recognition of a non-native protein and protein refolding. *EMBO J*. 1996;15:2969–2979.

27. Meacham GC, Patterson C, Zhang W, Younger JM, Cyr DM. The Hsc70 co-chaperone CHIP targets immature CFTR for proteasomal degradation. *Nat Cell Biol*. 2001;3:100–105.

28. Zhang H, Peters KW, Sun F, Marino CR, Lang J, Burgoyne RD, Frizzell RA. Cysteine string protein interacts with and modulates the maturation of the cystic fibrosis transmembrane conductance regulator. *J Biol Chem*. 2002;277:28948–28958.

29. Younger JM, Ren HY, Chen L, Fan CY, Fields A, Patterson C, Cyr DM. A foldable CFTR {Delta} F508 biogenic intermediate accumulates upon inhibition of the Hsc70-CHIP E3 ubiquitin ligase. *J Cell Biol*. 2004;167: 1075–1085.

30. Vila-Carriles WH, Zhou ZH, Bubien JK, Fuller CM, Benos DJ. Participation of the chaperone Hsc70 in the trafficking and functional expression of ASIC2 in glioma cells. *J Biol Chem*. 2007;282:34381–34391.

31. Guo J, Massaeli H, Xu J, Jia Z, Wigle JT, Mesaeli N, Zhang S. Extracellular K+ concentration controls cell surface density of I_{Kr} in rabbit hearts and of the HERG channel in human cell lines. *J Clin Invest*. 2009;119:2745–2757.

32. Nakamura H, Ding WG, Sanada M, Maeda K, Kawai H, Maegawa H, Matsuura H. Presence and functional role of the rapidly activating delayed rectifier K^+ current in left and right atria of adult mice. *Eur J Pharmacol*. 2010;649:14–22.

33. Karjalainen J, Viitasalo M. Fever and cardiac rhythm. *Arch Intern Med*. 1986;146:1169–1171.

34. Amin AS, Herfst LJ, Delisle BP, Klemens CA, Rook MB, Bezzina CR, underkofler HA, Holzem KM, Ruijter JM, Tan HL, January CT, Wilde AA. Fever-induced QTc prolongation and ventricular arrhythmias in individuals with type 2 congenital long QT syndrome. *J Clin Invest*. 2008;118:2552–2561.

35. Nuss HB, Marban E, Johns DC. Overexpression of a human potassium channel suppresses cardiac hyperexcitability in rabbit ventricular myocytes. *J Clin Invest*. 1999;103:889–896.

36. Royer A, Demolombe S, Harchi AE, Le Quang K, Piron J, Toumaniantz G, Mazurais D, Bellocq C, Lande G, Terrenoire C, Motoike HK, Chevallier JC, Loussouarn G, Clancy CE, Escande D, Charpentier F. Expression of human ERG K^+ channels in the mouse heart exerts anti-arrhythmic activity. *Cardiovasc Res*. 2005;65:128–137.

37. Choo-Kang LR, Zeitlin PL. Induction of HSP70 promotes DeltaF508 CFTR trafficking. *Am J Physiol Lung Cell Mol Physiol*. 2001;281:58–68.

38. Collawn JF, Bebok Z, Matalon. Search and rescue: finding ways to correct deltaF508 CFTR. *Am J Respir Cell Mol Biol*. 2009;40:385–387.

ilarities and interact with one another in an ATP-dependent fashion. *J Cell Biol*. 1993;120:1101–1112.

Novelty and Significance

What Is Known?

- The human ether-a-gogo-related gene (hERG) encodes the potassium channel α-subunit, I_{Kr}, and its hereditary dysfunction causes long QT syndrome type 2 (LQT2).
- Heat shock protein (Hsp)70 stabilizes hERG protein to increase I_{Kr}.
- Heat shock cognate (Hsc)70, because of its high degree of sequence homology to Hsp70, may also influence hERG protein.

What New Information Does This Article Contribute?

- We found that Hsc70 destabilizes hERG proteins to decrease I_{Kr}, indicating that Hsc70 and Hsp70 reciprocally control the maturation of hERG proteins. Hsp70 competes with Hsc70 in the binding with hERG and facilitates its maturation.

- Heat shock–induced Hsp70 increases the level of the mature form of missense mutant hERG causing LQT2.

The hERG channel plays an important role in cardiac electric activity. It has been shown that inherited mutations in hERG or pharmacological block of I_{Kr} increases the risk of lethal arrhythmia. Here, we show for the first time that Hsc70 and Hsp70 exert reciprocal effects on stability of hERG proteins. We also found that maturation of disease-causing missense mutant hERGs could be restored by a heat shock. Similar effect was achieved by Hsc70 knockdown through a suppression of Hsc70-degradation pathway. Our study provides a new insight into pathogenesis of inherited arrhythmia at the molecular and cellular levels and may lead to a novel therapeutic approach for treating arrhythmias.

SUPPLEMENTAL MATERIAL

Detailed Methods

Cell culture and transfection

HEK293 cells were cultured in DMEM (Sigma) supplemented with 10% fetal bovine serum (JRH) and penicillin/streptomycin/geneticin at 37°C, 5% CO_2.[14] HL-1 mouse cardiomyocytes were maintained as previously described.[5] An expression construct pcDNA3/hERG-FLAG was engineered by ligating an oligonucleotide encoding a FLAG epitope to the carboxy terminus of hERG cDNA. Missense mutations were introduced into pcDNA3/hERG-FLAG by site-directed mutagenesis (Figure 8A). pcDNA3 expression plasmid for Hsp70 was provided by A. Nakai and Hsc70 was a gift from Harm H. Kampinga (Groningen, Netherlands). The plasmids were transfected into HEK293 cells using lipofectamine 2000 (invitrongen) following the manufacturer's instructions. The total amount of cDNA was adjusted using vector cDNA. Transfection into HL-1 cells was performed using Nucleofector technology (Amaxa Biosystems, Gaithersburg, MD) following the manufacturer's protocol. For chase experiments, 48h after transfection, cycloheximide (60µg/ml) was added to the culture medium and cells were harvested at indicated time points.

Small interference RNA (siRNA)

Two active oligonucleotides against Hsp70 or Hsc70 and a scrambled control siRNA were used. Table 1 shows sequences of siRNA against Hsp70 and Hsc70. Cells were transfected with siRNA using lipofectamine 2000 (invitrogen) according to manufacturer's instructions.

Immunoblotting and immunoprecipitation

Cells were harvested 48h after transfection and lysed by sonication in a lysis buffer (PBS supplemented with 1% polyoxyethylene (9) octyiphenyl ether (NP-40), 0.5% sodium deoxycholate, 0.1% SDS, 1.5mmol/L aprotinin, 21mmol/L leupeptine, 15mmol/L pepstain and 1 mmol/L phenylmethylsulfonylfluoride). After removal of insoluble materials by centrifugation, protein concentrations were determined with a bicinchoninic acid (BCA) protein assay kit (Pierce, Biotechnology, Rockford, IL). Proteins were separated on SDS-PAGE and electrotransferred to PVDF membranes. The membranes were blocked with 5% non-fat dry milk in PBS plus 0.1% Tween and immunoblotted with a primary antibody. The following antibodies were used: FLAG epitope (Cosmo Bio), Hsp70 (mouse monoclonal; Stressgen), Hsc70 (Rat monoclonal; Stressgen), ubiquitin (Medical & Biological laboratory.Co. Ltd), calnexin (calbiochem), Na^+/K^+ ATPase (upstate), β-actin (Oncogene), GFP (Molecular Probes) and $hKv_{11.1}$ (HERG;Alomone Labs). The blots were developed by using an ECL system (Amersham, Biosciences, Piscataway, NJ). Immunoprecipitation was carried out at 4 °C for overnight in PBS supplemented with 1% Triton X-100, 0.5% SDS, 0.25% sodium deoxycholate, 1 mmol/L EDTA, and protease inhibitors. Immunocomplexes were collected with protein G agarose (Pharmacia, Uppsala, Sweden) and bound proteins were analyzed by SDS-PAGE followed by immunoblotting. Band densities were quantified using a NIH image J software. The all image densities of Western blotting were quantified and normalized to their image densities of ß-actin level.

Optiprep gradient cell fractionation

2

Cell fractionation was performed as described with a minor modification.[6] 48h after transfection, cells were collected by scraping in a medium (in mmol/L: sucrose 0.25, NaCl 140, EDTA 1, and Tris-HCl 20, pH 8.0) and homogenized by using a polytron. After removal of nuclei by centrifugation, the post-nuclear supernatants were layered onto a 10-40% liner gradient of iodixanolin cell fractionation buffer (Axis-Shild PoC, Oslo, Norway) and centrifuged at 48,000×g at 4°C for 22h using a Beckman SW41Ti rotor. 22 fractions (0.5 ml each) were collected from the top and were numbered accordingly. Immunoblot analyses were performed using antibodies against organelle markers and hERG-FLAG as indicated.

Immunofluorescence

HEK293 cells were seeded onto gelatin- coated coverslips and transfected with hERG-FLAG, pAcGFP-Golgi or pAcGFP-Mem constructs (Clontech) together with pcDNA3/Hsp70 or Hsc70. 24h after transfection, they were fixed with 4% paraformaldehyde/PBS and then permeabilized with 0.5% Triton X-100. They were incubated for 1h at room temperature with a primary antibody (FLAG, 1:1000; calnexin, 1:200). After blocking in 3% albumin, bound antibodies were visualized with AlexaFluor 546 or 488-conjugated mouse secondary antibody (1:2000), and images were obtained by using a Bio-Rad MRC 1024 confocal microscope. To quantify hERG-FLAG signals, the images of hERG-FLAG signals were cropped with regard to the distribution of each marker proteins (calnexin, Golgi-GFP and GFP1-Mem) using Photoshop CS3 software (Adobe Systems, US). The signal intensities in the cropped images were quantified by Image J software (NIH, US).

Establishment of WThERG-FLAG stable cell line

The plasmids of pcDNA3/hERG-FLAG were transfected into HEK293cells using lipofectamine 2000 following the manufacturer's instructions. The cells were divided 48hours after transfection and cultured at medium containing 1000μg/mL Geneticin (G418). We pick up 60 single clones to culture at the selecting medium for 7 weeks. The expressions of hERG-FLAG were confirmed by Western blot and membrane currents recorded by the whole-cell patch clamp technique showed typical properties of hERG channel currents.

Electrophysiological recordings

HEK293 cells stably expressing hERG-FLAG were transfected with pcDNA3/ Hsc70 or Hsp70 together with pEGFP. The total amount of cDNA was adjusted by vector cDNA. Twenty-four hours after transfection, cells were visualized by EGFP fluorescence and hERG channel currents corresponding to the rapidly-activating delayed-rectifer K^+ channel (I_{Kr}) currents were measured at 37°C using the whole-cell patch-clamp techniques with an Axopatch-200 amplifier (Axon instrument, USA). Procedures for the current measurement in HL-1 cells were essentially the same as described previously.[7] The extracellular solution contained (mmol/L) : NaCl 140, KCl 4, $CaCl_2$ 1.8, $MgCl_2$ 0.53, NaH_2PO_4 0.33, glucose 5.5, HEPES 5, pH was adjusted to7.4 by NaOH. The internal pipette solution contained (mmol/L) K-aspartate 100, KCl 20, $CaCl_2$ 1, Mg-ATP 5, EGTA 5, HEPES 5, creatine phosphate 5, dipotassium (pH 7.2 with KOH). 0.4μmol/L nisolddipine was included in the bath solution to block $I_{Ca,L}$.[8] The membrane potential was held at -50mV

3

to inactivate I_{CaT} and avoid I_f activation,[8,9] depolarized by 1-s test pulses (from -40mV to +40mV in 10mV increments), then repolarized back to the holding potential. Peak amplitudes of the currents during the depolarizing pulses and tail currents during the repolarization were determined and plotted as functions of the potentials of the depolarizing pulses. Action potentials were also measured in the current-clamp mode, elicited at a rate of 0.5 Hz by 5-ms square current pulses of 1nA, and sampled at 20 kHz in the absence or presence of 10 μmol/L E4031 (WAKO, Japan).

Semi-quantitative reverse transcription-PCR (RT-PCR)

Total RNAs were extracted from HEK293 cells using an RNeasy Plus mini kit (QIAGEN) and subjected to RT-PCR assay (Prime Scrips RT-PCR Kit, Takara). RNA samples were treated with DNase I (Promega) to eliminate genomic DNA. Primers used are;

hERG forward primer: CGCTACCACACACAGATGCT, reverse: GATGTCATTCTTCCCCAGGA,

β-actin forward primer: CAACCGTGAAAAGATGAC, reverse: CAGGATCTTCATGAGGTAGT.

PCR products were separated on electrophoresis gel, stained with ethidium bromide, and visualized in a UV transsilluminator.

Statistical analysis

All data are presented as the mean± SEM. For statistical analysis, Student's t-test and repeated measures analysis of variance (two-way ANOVA) were used, with $p < 0.05$ being considered statistically significant.

4
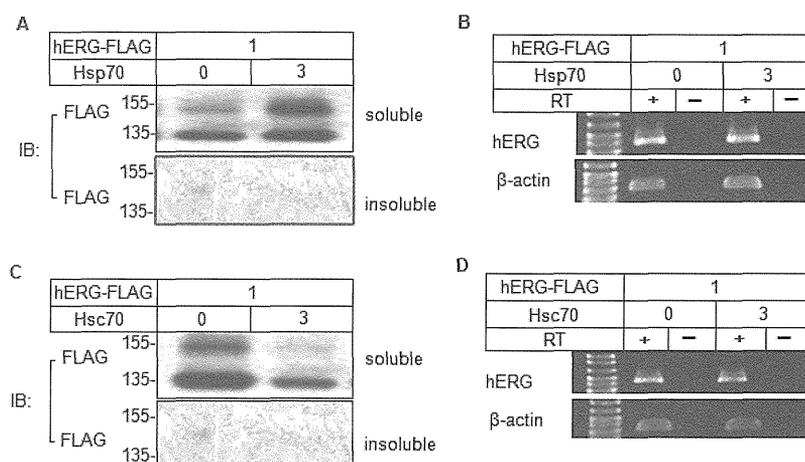
Online Figure I

Online Figure I. Effects of Hsp70 or Hsc70 on protein solubility and transcriptional expression of hERG.
HEK293 cells were transiently expressed with hERG-FLAG, GFP and either Hsp70 (**A**) or Hsc70 (**C**) plasmid. The soluble and insoluble fractions of cell lysates were subjected to Western blotting against anti-FLAG antibody.
B and D, Semi-quantitative reverse transcription-PCR (RT-PCR) of hERG mRNA expressed in HEK293 cells (+). β-actin levels were analyzed as control. No band was detected from PCR amplification of RNA without RT (-).
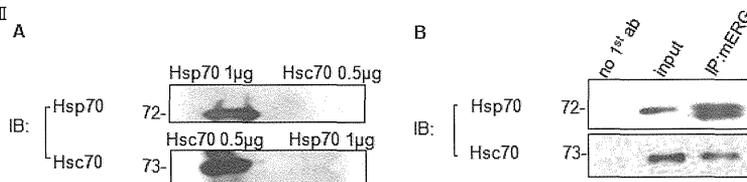
5

— 48 —
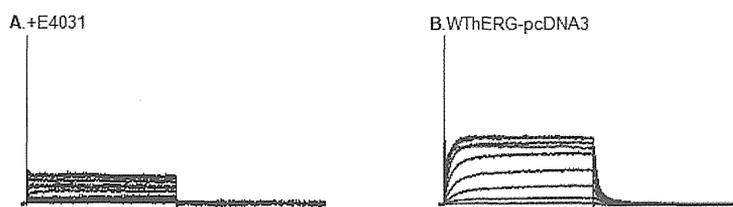
Online Figure II

Online Figure II. E4031 inhibited hERG currents.

A, A representative trace of whole-cell current mediated by hERG-FLAG in presence of E4031.

B, A representative trace of whole-cell current mediated by hERG-pcDNA3.
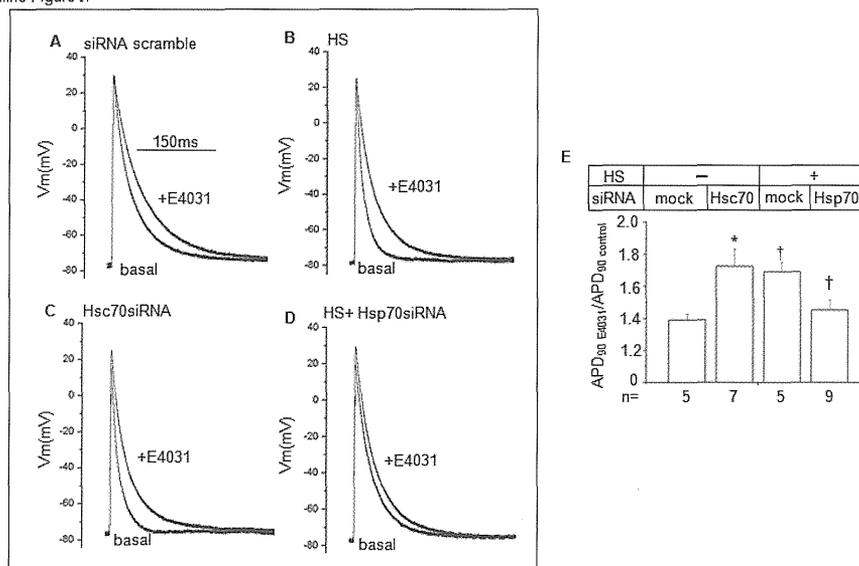
Online Figure III

Online Figure III. Bindings of Hsp70 or Hsc70 with endogenous mouse ERG (mERG).

A, Confirmation of the specificity of Hsp70 and Hsc70 antibodies.

Anti-Hsp70 and Hsc70 antibodies were conducted to detect Hsp70 or Hsc70 recombinant proteins by Western blot, respectively.

B, Anti-mERG immunoprecipitates from HL-1 cell lysates were subjected to immunoblotting with anti-Hsp70 or Hsc70 antibody, respectively. Negative control (no 1st ab) and positive control (input) were applied in the first and second lanes.

6

Online Figure IV

Online Figure IV. The effects of E4031 on APD in HL-1 cells.

Left panel (**A-D**) shows representative action potentials recorded for the indicated groups in the absence or presence of E4031. Bar graphs on the right (**E**) summarize the percentage of APD_{90} prolongation ($APD_{90\ E4031}/APD_{90\ control}$) by E4031 treatment. * $p<0.05$, † $p<0.01$ vs a scramble siRNA control with non-HS treatment; ‡ $p<0.05$ vs a scramble siRNA control with the HS treatment.

Table I, Sequences of siRNA

	sense	antisense
Human Hsp70-2	5'-TCCTGTGTTTGCAATGTTGAATT-3'	5'-UUCAACAUUGCAAACACAGGATT-3'
Human Hsp70-3	5'-TTCAAAGTAAATAAACTTTAATT-3'	5'-UUAAAGUUUAUUUACUUUGAATT-3'
Human Hsc70-2	5'-CCGAACCACUCCAAGCUAUTT-3'	5'-AUAGCUUGGAGUGGUUCGG TT-3'
Human Hsc70-3	5'-CUGUCCUCAUCAAGCGUAATT-3'	5'-UUACGCU UGAUGAGGACAGTT-3'
Mouse Hsp70-1	5'-CUGGAGAUCGACUCUCUGUUC-3'	5'-ACAGAGAGUCGAUCUCCAGGC-3'
Mouse Hsp70-2	5'-CAGUCCGACAUGAAGCACUGG-3'	5'-AGUGCUUCAUGUCGGACUGCA-3
Mouse Hsc70-1	5'-CCGCACCACGCCAAGCUAUGU-3'	5'-AUAGCUUGGCGUGGUGCGGUU-3'
Mouse Hsc70-2	5'-CUAUUGCUUACGGCUUAGAUA-3	5'-UCUAAGCCGUAAGCAAUAGCA-3'

Supplemental References

1. Kato M, Ogura K, Miake J, Sasaki N, Taniguchi S, Igawa O, Yoshida A, Hoshikawa Y, Murata M, Nanba E, Kurata Y, Kawata Y, Ninomiya H, Morisaki T, Kitakaze M, Hisatome I. Evidence for proteasomal degradation of Kv1.5 channel protein. *Biochem. Biophys. Res. Commun.* 2005;337:343-348

7

2. Tanaka H, Miake J, Notsu T, Sonyama K, Sasaki N, Iitsuka K, Kato M, Taniguchi S, Igawa O, Yoshida A, Shigemasa C, Hoshikawa Y, Kurata Y, Kuniyasu A, Nakayama H, Inagaki N, Nanba E, Shiota G, Morisaki T, Ninomiya H, Kitakaze M, Hisatome I. Proteasomal degradation of Kir6.2 channel protein and its inhibition by a Na+ channel blocker aprindine. *Biochem Biophys Res Commun*. 2005;331:1001-1006.

3. Hirota Y, Kurata Y, Kato M, Notsu T, Koshida S, Inoue T, Kawata Y, Miake J, Bahrudin U, Li P, Hoshikawa Y, Yamamoto Y, Igawa O, Shirayoshi Y, Nakai A, Ninomiya H, Higaki K, Hiraoka M, Hisatome I. Functional stabilization of Kv1.5 protein by Hsp70 in mammalian cell lines. *Biochem Biophys Res Commun*. 2008;372:469-474.

4. Koshida S, Kurata Y, Notsu T, Hirota Y, Kuang TY, Li P, Bahrudin U, Harada S, Miake J, Yamamoto Y, Hoshikawa Y, Igawa O, Higaki K, Soma M, Yoshida A, Ninomiya H, Shiota G, Shirayoshi Y, Hisatome I. Stabilizing effects of eicosapentaenoic acid on Kv1.5 channel protein expressed in mammalian cells. *Eur J Pharmacol*. 2009;604:93-102.

5. Claycomb WC, Lanson NA Jr, Stallworth BS, Egeland DB, Delcarpio JB, Bahinski A, Izzo NJ Jr. HL-1 cells: a cardiac muscle cell line that contracts and retains phenotypic characteristics of the adult cardiomyocyte. *Proc Natl Acad Sci U S A*. 1998;95:2979-2984.

6. Woods AJ, Robert MS, Choudhary J, Barry ST, Mazaki Y, Sabe H, Morley SJ, Critchley DR, Norman JC. Paxillin associates with poly (A)-binding protein 1 at the dense endoplasmic reticulum and the leading edge of migrating cells. *J Biol Chem*. 2002;277:6428-6437.

7. Toyota F, Ding WG, Zankov DP, Omatsu-Kanbe M, Isono T, Horie M, Matsuura H. Chearaterization of the rapidly activating delayed rectifier potassium current, I_{Kr}, in Hl-1 mouse atrial myocytes. *J membrane Biol*. 2010;235:73-87.

8. Xia M, Salata JJ, Figueroa DJ, Lawlor AM, Liang HA, Liu Y, Connolly TM. Functional expression of L- and T-type Ca2+ channels in murine HL-1 cells. *J Mol Cell Cardiol*. 2004;36:111-119.

9. Sartiani L, Bochet P, Cerbai E, Mugelli A, Fischmeister R. Functional expression of the hyperpolarization-activated, non-selective cation current I(f) in immortalized HL-1 cardiomyocytes. *J Physiol*. 2002;545:81-92.

8

ORIGINAL ARTICLE
Arrhythmia/Electrophysiology

Risk Determinants in Individuals With a Spontaneous Type 1 Brugada ECG

Akashi Miyamoto, MD; Hideki Hayashi, MD, PhD; Takeru Makiyama, MD, PhD;
Tomohide Yoshino, MD; Yuka Mizusawa, MD; Yoshihisa Sugimoto, MD, PhD;
Makoto Ito, MD, PhD; Joel Q Xue, PhD; Yoshitaka Murakami, PhD; Minoru Horie, MD, PhD

Background: Spontaneous coved ST-segment elevation ≥2 mm followed by a negative T-wave in the right precordial leads (type 1 Brugada ECG) is diagnostic of Brugada syndrome (BS), but there is a false-positive rate.

Methods and Results: Computer-processed analysis of a 12-lead ECG database containing 49,286 females and 52,779 males was performed to select patients with a spontaneous type 1 Brugada ECG for an examination of the association of this ECG characteristic with long-term prognosis. There were 185 patients with a spontaneous type 1 Brugada ECG and of these, 16 (15 males; mean age, 46.7±14.0 years) were diagnosed with BS and 15 patients (all males; mean age, 50.1±13.4 years) were undiagnosed. The PQ interval was significantly longer in the diagnosed patients than in the undiagnosed patients (187.4±28.3 ms vs. 161.2±21.5 ms; P=0.0073). The T-wave in lead V_1 was more negative in the diagnosed patients than in the undiagnosed patients (−170.2±174.6 μV vs. −43.2±122.3 μV, P=0.027). Multivariate analysis revealed that a PQ interval ≥170 ms and T-wave amplitude <−105 μV in lead V_1 were independent risk stratifiers of life-threatening events. Survival analysis (mean follow-up, 78.6±81.8 months) showed that the PQ interval and a negative T-wave in lead V_1 were significantly associated with poor prognosis.

Conclusions: Analysis of a standard 12-lead ECG can stratify the prognosis of patients with a spontaneous type 1 Brugada ECG. (*Circ J* 2011; **75:** 844–851)

Key Words: Brugada syndrome; Electrocardiography; Prognosis; Risk determinant; Sudden death

Brugada syndrome (BS) is characterized by a distinct ST-segment elevation in the right precordial leads and causes sudden cardiac death.[1] This syndrome has a relatively high prevalence in East Asian countries. Patients with a coved-type ST-segment elevation in leads V_{1-3} are more susceptible to life-threatening ventricular arrhythmias than patients with a saddleback-type ST-segment elevation in the same leads.[2] A community-based study reported that subjects who displayed a spontaneous coved ST-segment elevation in the right precordial leads were not at risk for sudden death,[3] but another study, in which the mean follow-up period was >40 years, reported that an ECG with a coved ST-segment elevation was related to an increased risk of unexplained death.[4] Similar inconsistency has been found among studies conducted in hospital-based populations.[5–7] The discrepancy indicates that a distinct coved ST-segment elevation may not be the sole determinant of prognosis.

Editorial p 777

To stratify prognostic risk in BS, pharmacological and electrophysiological tests are performed, but the prognostic value of these tests is yet to be settled.[8,9] In addition, mutation of the gene that encodes the cardiac sodium channel, *SCN5A*,[10] is detected only in approximately 20% of patients diagnosed with BS,[6] suggesting that it may be difficult to screen out subjects who are at high risk for lethal arrhythmia by genetic testing alone.

The large database of a university hospital containing 12-lead ECGs of more than 100,000 patients stored digitally for over 25 years, enabled us to evaluate long-term prognosis using computer-processed analysis. Since 12-lead ECG is the most convenient method of diagnosing BS in a large population, such as in health examinations, in the present

study we focused on patients with a spontaneous coved ST-segment elevation ≥0.2mV in the right precordial leads (ie, type 1 Brugada ECG). Our aim was to determine the quantitative traits of a spontaneous type 1 Brugada ECG that can stratify the risk for sudden cardiac death (SCD).

Methods

Database
The database comprised 102,065 consecutive patients (49,286 females and 52,779 males) who had undergone ECG recording in the university hospital between January 1983 and October 2008. A total of 308,391 ECGs were collected during this period. The 12-lead ECG was recorded at rest for 10s at a sweep speed of 25mm/s, calibrated to 1mV/cm in the standard leads. The data were digitally stored in a 12-bit server computer with a sampling interval of 2ms.

Patient Population
From the database, we chose patients who had a spontaneous coved ST-segment elevation in the right precordial leads. We enrolled patients who fulfilled the following ECG criteria: (1) J-point elevation ≥0.2mV amplitude in lead V_1 or V_2, (2) the amplitude at the middle of the ST-segment (STM: defined as the time point after an interval of 1/16 of the average RR interval from the J point) in lead V_1 or V_2 was less than that at the J point in the same lead, (3) the amplitude at the end of the ST-segment (defined as the time point after an interval of 1/8 of the average RR interval from the J point) in lead V_1 or V_2 was less than that at the middle of the ST-segment in the same lead, and (4) the amplitude at the J point and the middle of the ST-segment was positive in leads V_1 and V_2. The J point was defined as the offset of the QRS complex that was the latest detection of ventricular depolarization. To exclude right bundle branch block, we did not include any ECG that displayed the QRS complex in lead V_1 with a decrease in amplitude of ≥0.4mV from the J point.

ECG Analysis
The ECG analysis was performed using software (MUSE7.1, GE Marquette Medical Systems, Inc, Milwaukee, WI, USA). ECG variables, including duration, interval, amplitude, and axis, were digitally measured. A median complex was computed as follows: (1) all QRS complexes with the same morphology were aligned in time and (2) the algorithm generated a representative QRS complex from the median voltages that were found at each successive sample time. QRS duration was measured from the earliest detection of depolarization in any lead (QRS onset) to the latest detection of depolarization in any lead (QRS offset). Similarly, the QT interval was measured from the earliest detection of depolarization in any lead (QRS onset) to the latest detection of repolarization where the downsloping limb joined the baseline in any lead (T offset), while the U wave was excluded. The QTc interval was calculated after correction for heart rate with Bazett's formula. The frontal plane angle of the P wave, QRS complex, and T wave was determined from the frontal leads (I, II, III, aVR, aVL, and aVF). The frontal plane QRS–T angle was defined as the absolute value of the difference between the frontal planes of the QRS axis and T axis, and was adjusted to the minimal angle using "360° minus the angle" for an angle >180° (axis measurement range; –89° to +270°). Because all variables of the 12-lead ECG were digitally measured by computer-processed analysis, neither intra-observer nor interobserver variability was taken into account.

Follow-up
The follow-up period of all patients was defined as the interval from the first day when a spontaneous type 1 Brugada ECG was recorded to the day when prognostic outcome was identified. The prognostic value was assessed for the endpoint of documented ventricular fibrillation (VF) or sustained ventricular tachycardia (VT) that was either symptomatic or revealed by an implanted device. A postal questionnaire was used to assess the prognosis of patients who were not associated with the Division of Cardiology in the hospital. Written informed consent was given by all patients enrolled in this study.

Diagnosis
When a spontaneous type 1 Brugada ECG was present, BS was diagnosed on the basis of a consensus report requiring at least one of the following criteria: documented VF, self-terminating polymorphic VT, family history of sudden death, type 1 Brugada ECG in family members, positive electrophysiological study, unexplained syncope suggestive of ventricular tachyarrhythmia, and nocturnal agonal respiration.[2] Confounding factors[1] that have been previously reported as disorders accounting for a type 1 Brugada ECG were excluded. Drug-induced Brugada-like ECG pattern[2] was also excluded.
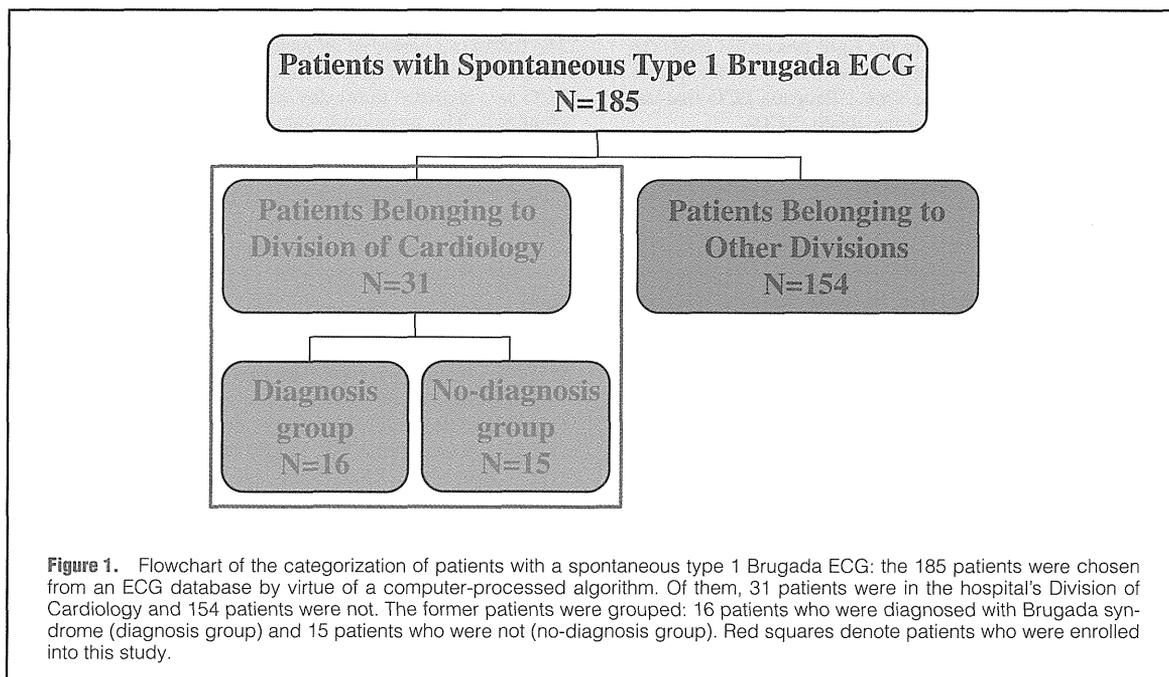
Gene Analysis
The methods of DNA isolation and mutation analysis are described elsewhere.[11] Briefly, genomic DNA was isolated from blood lymphocytes and then screened for candidate genes using denaturing high-performance liquid chromatography with a WAVE System Model 3500 (Transgenomic, Omaha, NB, USA). Polymerase chain reaction was used to amplify abnormal conformers, and sequencing was performed on an ABI PRISM 3100 DNA sequencer (Applied Biosystems, Foster City, CA, USA).

Statistical Analysis
We explored the prognostic factors for developing life-threatening events and the endpoint was the occurrence of life-threatening events. Continuous variables are reported as mean±SD and categorical variables as observed number of patients (percentage). We compiled 2 groups: patients who were diagnosed with BS (diagnosis group) and patients who were not diagnosed with BS (no-diagnosis group). In the comparison of their clinical and ECG characteristics, we used a t-test for continuous variables and Fisher's exact test or χ^2 test for categorical variables. Receiver-operating characteristic curve was used to determine the optimal cut-off point of the prognostic factors that maximizes the sensitivity and specificity of ECG variables for the diagnosis of BS. Logistic regression was used to compare the patients with/without BS to explore the prognostic factors accounting for confounding. The forward selection procedure was applied for the selection of variables in the logistic regression and the criteria was set as P<0.10. For the significant variables in the model, the Kaplan-Meier curve was made to describe the event-free survival rate and the log-rank test was used to examine the difference between 2 groups. All tests were 2-tailed and the significance level was set as 0.5. The research protocol was approved by the Ethical Committee of Shiga University of Medical Science (19–75).

Results

We located 185 patients who fulfilled the ECG criteria of a

Figure 1. Flowchart of the categorization of patients with a spontaneous type 1 Brugada ECG: the 185 patients were chosen from an ECG database by virtue of a computer-processed algorithm. Of them, 31 patients were in the hospital's Division of Cardiology and 154 patients were not. The former patients were grouped: 16 patients who were diagnosed with Brugada syndrome (diagnosis group) and 15 patients who were not (no-diagnosis group). Red squares denote patients who were enrolled into this study.

Table 1. Characteristics of the Patients With Spontaneous Type 1 Brugada ECG

	Diagnosis group	No-diagnosis group	P value
No. of patients	16	15	
Age (years)	46.7±14.0	50.1±13.4	0.50
Male (n, %)	15 (93.8)	15 (100)	0.24
Follow-up period (months)	58.5±75.1	43.2±42.7	0.49
Family history of SCD (n, %)	8 (50.0)	0 (0)	0.0008
Syncope (n, %)	14 (87.5)	3 (20.0)	<0.001
Aborted SCD or documented VF (n, %)	11 (68.8)	0 (0)	<0.001

SCD, sudden cardiac death; VF, ventricular fibrillation.

spontaneous type 1 Brugada ECG in the database (**Figure 1**). The prevalence of a spontaneous type 1 Brugada ECG was 0.18% of the total patients who underwent ECG recording in the hospital. Of the 185 patients, 31 attended the Division of Cardiology: 16 patients were diagnosed as BS (diagnosis group) and 15 patients were not (no-diagnosis group). Representative ECGs are shown in **Figures S1 and S2**. All the patients of the diagnosis and no-diagnosis groups were carefully followed in the Division of Cardiology. The remaining 154 patients who had exhibited a spontaneous type 1 Brugada ECG attended other divisions of the hospital and had undergone ECG recording irrespective of cardiovascular disease (eg, before surgery). The mean follow-up of the 2 groups was 51.1±61.1 months, ranging from 1 to 238 months.

Characteristics of the Patients

The detailed clinical characteristics of each group are shown in **Table 1**. The mean age of each group was not significantly different, the male predominance was similar between the 2 groups and the mean follow-up period was not significantly different between the 2 cohorts. In the diagnosis

group, 14 of the 16 patients diagnosed with BS suffered syncope, and in 12 of the 14 patients, lethal ventricular arrhythmias (VF or VT) were documented. Although the remaining 2 patients did not have a documented episode of lethal arrhythmias, both patients had syncopal episodes considered to be of arrhythmic origin. In those 2 patients, VF was induced by programmed ventricular stimulation. An implantable cardioverter-defibrillator (ICD) was implanted in all patients but 1 patient who rejected the procedure. After ICD implantation, 6 patients experienced VF. In the diagnosis group 8 patients (50%; 1 female, 7 males) had a family history of sudden death. In the no-diagnosis group, the 15 patients, who had been referred to the Division of Cardiology, displayed a spontaneous type 1 Brugada ECG but were not diagnosed as BS because none suffered from unexplained syncope or had a family history of SCD. Therefore, it was not considered necessary to implant ICDs in these patients, but they were required to visit hospital regularly for health checks. In the no-diagnosis group, 3 patients experienced syncope that was most likely due to a neurally mediated mechanism, because precipitating events, such as severe